Hutnické listy – *Metallurgical Journal*
Speciální vydání / Special Issue, roč. / vol. LXXIX
ISSN Online: 3029-8350

Hydrogen Removal during RH Degassing of Molten Steel: Real-Time Recurrence CFD Predictions and Validation using Plant Data

Odstraňování vodíku během odplynění oceli procesem RH: Predikce v reálném čase pomocí CFD modelu a jeho validace využitím provozních údajů

Xiaomeng Zhang[1], Maria Thumfart[1], Johann Wachlmayr[1], Christine Gruber[1], Roman Rössler[2], Daniel Queteschiner[3], Stefan Pirker[3]

[1] K1-MET GmbH, Linz, Austria. *Contact e-mail: Xiaomeng.zhang@k1-met.com
[2] voestalpine Stahl GmbH, Linz, Austria
[3] Department of Particulate Flow Modelling, Johannes Kepler University, Linz, Austria

Abstract

In this study, data-assisted recurrence CFD (rCFD) is applied to efficiently simulate hydrogen degassing of molten steel in the RH vacuum process over time spans of tens of minutes. To ensure that numerical predictions are directly comparable to the hydrogen measured in the far-end off-gas stream at the plant, a transfer function is developed based on plant data, specifically, according to the relationship between injected lift-gas and its corresponding output in the off-gas. This function accounts for time delay and mixing effects as the gas reaches the monitoring point in the plant.

Initial comparisons show that rCFD predictions of hydrogen removal qualitatively agree well with plant data while enabling real-time predictions. To achieve quantitative agreement, further efforts are required to address uncertainties in hydrogen mass loss in off-gas measurement and to improve the model implementation in rCFD, particularly the calculation of hydrogen partial pressure. With validation established through plant data, rCFD's real-time predictive capability renders it a promising tool for three-dimensional digital twin applications in the RH process.

***Keyword**: RH plant, CFD, recurrence CFD, hydrogen degassing*

Abstrakt

V této studii je využita metoda datově podporované rekurentní CFD (rCFD) k efektivní simulaci odstranění vodíku z roztavené oceli v RH vakuovém procesu odplynění v časovém horizontu desítek minut. Aby bylo zajištěno, že numerické predikce jsou přímo srovnatelné s koncentrací vodíku měřenou ve výstupním proudu odtahového plynu, byla na základě provozních dat navržena přenosová funkce, vycházející ze vztahu mezi vstřikovaným zdvihovým (nosným) plynem a jeho odezvou v odtahovém plynu. Tato funkce zohledňuje časové zpoždění a mísicí efekty při transportu plynu k místu měření.

Počáteční srovnání ukazují, že predikce rCFD týkající se odstraňování vodíku jsou v kvalitativní shodě s provozními daty a současně umožňují predikce v reálném čase. Pro dosažení kvantitativní shody je však nutné dále řešit nejistoty spojené s měřením úbytku vodíku v odtahovém plynu a zpřesnit implementaci modelu v rCFD, zejména výpočet parciálního tlaku vodíku. Díky validaci na základě provozních dat a schopnosti predikce v reálném čase představuje rCFD perspektivní nástroj pro aplikace trojrozměrných digitálních dvojčat v RH procesu.

***Klíčová slova:** RH vakuovací stanice, výpočetní dynamika tekutin CFD, rekurentní CFD (rCDF), odstranění vodíku*

Hutnické listy – *Metallurgical Journal*
Speciální vydání / Special Issue, roč. / vol. LXXIX
ISSN Online: 3029-8350

1. Introduction

With the growing demand for sustainable steel production, enhancing the efficiency and precision of control in secondary refining processes, such as the Ruhrstahl-Heraeus (RH) process, has become increasingly critical to the steel industry. Due to the demanding process conditions (high temperatures, opaque liquids, and thick walls), CFD simulations have been an essential tool to better access and provide detailed three-dimensional insights into the fluid flow and mixing phenomena in the RH process. The turbulent and multiphase flow (particularly the interaction of rising bubble plumes and liquid steel) features in the process have been addressed by different models with varying levels of complexity [1-5]. A comprehensive review by Chen et al. [6] summarized recent progress in CFD modelling of argon-steel(-slag) multiphase flow in the RH process, covering aspects such as bubble dynamics, turbulence models, multiphase interactions, and validation techniques.

However, the high computational cost of conventional CFD simulations limits their application to short-term, offline analyses, making them unsuitable for real-time online process monitoring. To overcome this limitation, Lichtenegger and Pirker [7] proposed a fast simulation technique known as recurrence CFD (rCFD). This data-assisted methodology uses a database of characteristic flow patterns generated by conventional short-term CFD simulations and subsequently time-extrapolates these data to industrial process times. Without the need to solve the governing equations at each time step, rCFD dramatically reduces computational time, enabling real-time or even faster than real-time simulations of various industrial-scale cases such as steelmaking converter, ladle and tundish [7-9] and fluidized beds [10–12] as well as pollutant dispersion in built environments [13].

In this study, we apply transport-based rCFD [8] to efficiently simulate long-duration hydrogen degassing in an industrial RH plant. The simulation results are compared with plant off-gas hydrogen measurements to assess the model's predictive capability. Furthermore, we discuss the potential to quantitatively align simulation and plant data by addressing uncertainties in both the numerical model and measurement system. This work is part of an ongoing effort to calibrate and validate a real-time-capable simulation tool using plant data, with the long-term goal of supporting online process monitoring and control.

2. Modelling and Simulation

The overall workflow for (transport-based) rCFD simulations is outlined below. A more detailed description of the rCFD methodology can be found in [7, 8].

As a data-assisted method, rCFD simulation generally starts with conducting a conventional CFD simulation until the given process exhibits pseudo-periodic flow characteristics. Then, a recurrence database covering a limited process duration is generated from the CFD simulation. Finally, the transport of passive scalars (e.g., removal of hydrogen) can be simulated over any arbitrary long process time by utilizing the database.

In the context of gas-injection-driven circulating flow in the RH process, the initial CFD simulation employs a combination of: (1) the VOF method for the steel surface motion in the vacuum chamber, (2) the DPM model for the injected gas bubbles from the up-leg snorkel, and (3) LES approach for turbulence modelling.

Hutnické listy – *Metallurgical Journal*
Speciální vydání / Special Issue, roč. / vol. LXXIX
ISSN Online: 3029-8350

The modelling strategy is commonly adopted for bubble plume-induced flow and has delivered reasonable results in comparison with experimental studies and plant observations [1, 14]. For brevity, the CFD modelling details are omitted here and can be found in the references [1, 14].

Once the steel flow reaches pseudo-periodic states, a continuation of CFD simulations of such flow spanning a monitoring period τ_{rec} feed a recurrence database that is subsequently used for long-duration simulations. There are currently two main versions of rCFD, labeled flow-based rCFD and transport-based rCFD. For the flow-based version of rCFD, the entire flow field is stored in a regular time interval Δt_{rec} over the period τ_{rec} (resulting in the number of N_{rec} instant flow fields or data frames). With these flow fields, a recurrence analysis is performed based on a recurrence norm (rNorm), which is a scalar quantity that quantifies the system's degree of similarity at two different times (here, rNorm is linked to the fluid velocity). Applying rNorm to each pair of these N_{rec} data frames results in a recurrence matrix (rMatrix) with N_{rec}^2 entries. The graphical representation of a rMatrix refers to a recurrence plot (as given by **Fig. 1(b)**), which always has a zero main diagonal as the frame is compared to itself and contains non-zero off-diagonal entries indicating whether two data frames are similar or not. Based on this information, a recurrence process (rProcess) can be constructed by stitching these flow sequences, with an emphasis on connecting similar states. For instance, starting at a certain time (or a certain data frame N_m), the subsequent ξ frames (ξ denotes a randomly chosen interval) are used consecutively. At frame $N_{m+\xi}$, frame N_n, which is the most similar to the current frame, is determined as the connecting frame. Then, having N_n as the starting frame, same method is applied to look for the next frame that fits the previous sequence's end frame. This process can be repeated to obtain an arbitrarily long flow sequence. Then, passive scalars are traced on the extrapolated flow fields by solving transport equations. In contrast to flow-based rCFD, the transport-based rCFD doesn't store flow fields themselves.

Rather, an additional field transport equation is solved which essentially tracks the advection of cell coordinates. These advected cell coordinates are subsequently transformed into a series of cell-to-cell shifts which then constitutes the database. Based on these cell-to-cell shifts a passive scalar quantity is propagated from the very frame's start cells to the receiving end cells in each time step (following the rProcess described previously).

In addition to cell shifts, face swaps among neighbouring cells are adopted to mimic physical diffusion in order to get smooth and complete field information. The transport-based rCFD has shown further computational speed-up compared to the flow-based rCFD and is used in this study. The rCFD functionalities are implemented within the framework of ANSYS Fluent via UDFs.

In applying the transport-based rCFD to hydrogen degassing, the degassing rate under vacuum condition can be described by a first-order reaction model given by Equation (1), considering the mass transfer of [H] in the boundary layer of molten steel the rate-controlling step.

$$-\frac{dm_{[H]}}{dt} = \rho A k_{[H]}([H] - [H]_e) \quad (1)$$

In the above equation, ρ is the steel density, A is reaction area between molten steel and the gas phase and $k_{[H]}$ is mass transfer coefficient with unit m/s. [H] and $[H]_e$ are mass fractions of [H] in steel and at surfaces (also equals to equilibrium content of element).

Hutnické listy – *Metallurgical Journal*
Speciální vydání / Special Issue, roč. / vol. LXXIX
ISSN Online: 3029-8350

$$K_{\mathrm{H}}^{\ominus} = \frac{\left(P_{\mathrm{H_2}}/P^{\ominus}\right)^{\frac{1}{2}}}{f_{[\mathrm{H}]}[\%\mathrm{H}]_{\mathrm{e}}} \tag{2}$$

$$\lg K_{\mathrm{H}}^{\ominus} = 1905/T + 1.591 \tag{3}$$

To implement Equation (1), the reaction area, mass transfer coefficient, and the equilibrium concentration are to be determined. The equilibrium content depends on the partial pressure of the reaction product H_2 and the thermodynamic equilibrium constant $K_{\mathrm{H}}^{\ominus}$ according to Equation (2) (the activity coefficient ($f_{[\mathrm{H}]}$) set to 1 for low-alloyed steels). The equilibrium constant is calculated by Equation (3) [15]. The mass transfer coefficient of hydrogen in molten steel is taken to be $k_{[\mathrm{H}]} = 1.42 \times 10^{-3}\mathrm{m.s^{-1}}$ [15]. Regarding reaction sites, this study assumes that the reaction primarily occurs in the vacuum chamber, supported by plant observations of the melt surface obtained from a high-speed camera, which reveals the presence of highly dynamic steel foam [16]. Given the much larger steel volume in the vacuum chamber compared to the up-leg snorkel, along with the high void fraction in the melt, a sufficiently large steel-gas interface is available. This, in turn, promotes an efficient degassing reaction in the vacuum chamber. The results of hydrogen degassing predicted by rCFD are presented subsequently.

3. Results and Discussion

The CFD simulation of the flow field in the RH plant, based on the modelling strategy described in the previous section, is shown in **Fig. 1(a)**. The characteristic recirculating flow pattern, driven by the injected bubbles at the up-leg snorkel, is well captured by the model. Once the flow structure is established, its dynamic behavior is further analysed using a recurrence plot, as presented in **Fig. 1(b)**. This plot visualizes the pairwise differences between frames for a total of 200 frames, covering a 20s process duration.

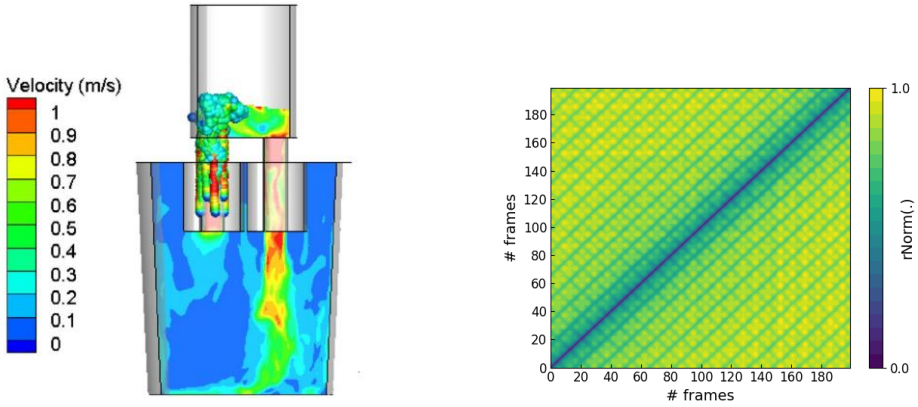

(a) (b)

Fig. 1 (a) Characteristic circulating flow topology in the RH plant obtained from CFD simulations. (b) Recurrence plot of the global flow field, constructed from 200 data frames and evaluating the flow evolution over a 20s process duration. The color scale indicates the degree of pairwise similarity: dark blue indicates identical frames, while yellow represents the greatest dissimilarity between frames

Obr. 1 (a) Charakteristika cirkulace proudění na vakuovací stanici RH získaná z CFD simulací. (b) Graf rekurentního pole proudění, sestavený z 200 datových snímků a zachycující vývoj proudění během 20sekundového procesu. Barevná stupnice udává míru párové podobnosti: tmavě modrá barva označuje identické snímky, zatímco žlutá barva představuje největší odlišnost mezi snímky

Hutnické listy – *Metallurgical Journal*
Speciální vydání / Special Issue, roč. / vol. LXXIX
ISSN Online: 3029-8350

Obviously, a zero-valued antidiagonal is present since it represents the comparison of a state with itself, resulting in no difference. In the off-diagonal region, distinct greenish parallel lines appear at constant intervals, indicating the periodic recurrence of similar flow states in the system. This recurrence behavior enables us to proceed with rCFD time extrapolation, as introduced earlier, and thereby efficiently simulate long-duration hydrogen degassing in the steel.

Fig. 2 shows the evolution of hydrogen concentration in the steel at three-time instances (t = 7, 15, and 23min), as predicted by rCFD simulations. The contour plots clearly show that hydrogen degassing initiates in the vacuum chamber, with hydrogen-depleted steel re-entering the ladle by a downward jet.

Through global steel recirculation, dissolved hydrogen is gradually washed out of the ladle, eventually reaching a low concentration. In addition, the computational cost associated with rCFD simulation of hydrogen degassing is also presented in **Fig. 2**.

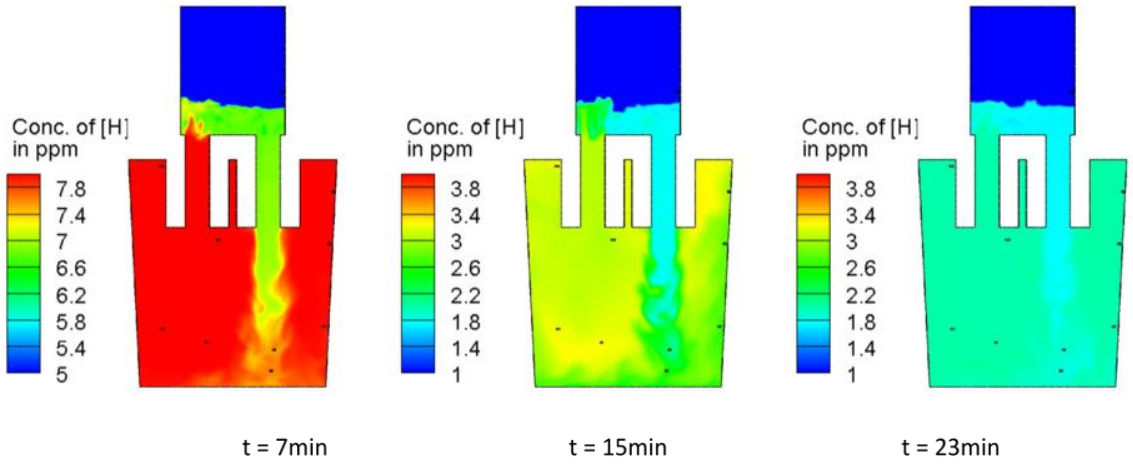

Computational efficiency of rCFD for hydrogen degassing

$t_{process}$	t_{CPU}
35min	45min (rCFD run)

Fig. 2 Instantaneous hydrogen [H] concentration in the steel at three-time instances obtained from rCFD simulations, along with the corresponding computational efficiency of rCFD

Obr. 2 Okamžitá koncentrace vodíku [H] v oceli ve třech časových okamžicích získaná z rCFD simulací spolu s odpovídající výpočetní účinností rCFD

The rCFD approach enables simulations at full grid resolution (2.5 million cells) with near real-time performance relative to the physical process time, which is not achievable using conventional full CFD simulations.

In addition to the time evolution of hydrogen concentration in the steel, the H_2 mass flow rate predicted by rCFD is compared with plant measurements of H_2 in the off-gas.

Since the simulation provides H_2 mass flow at the melt surface, while the measurements are taken at the far end of the off-gas pipeline, a transfer function is developed based on a specific type of plant treatment and applied to the simulation results. This function accounts for gas transport and mixing effects within the off-gas system.

Hutnické listy – *Metallurgical Journal*
Speciální vydání / Special Issue, roč. / vol. LXXIX
ISSN Online: 3029-8350

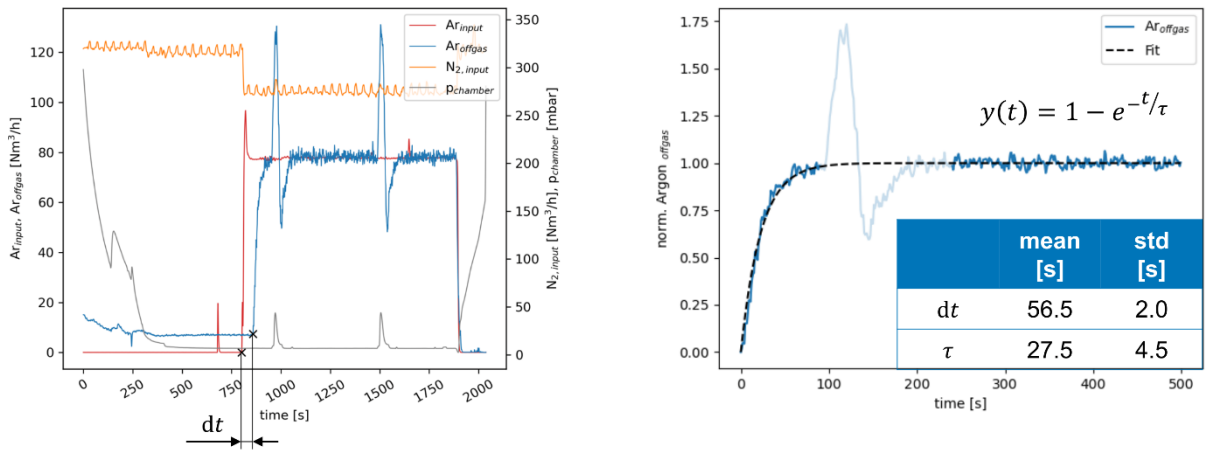

(a) (b)

Fig. 3 (a) RH operation with a lift-gas switch from N_2 to Ar: the Ar flow rate in the off-gas (blue line) exhibits a time-delayed and smoother response compared to the lift-gas signal (red line), due to gas transport and mixing within the off-gas system. (b) Fitted curve of the normalized Ar flow rate measured in the off-gas [16]

Obr. 3 Provoz RH stanice se změnou nosného plynu z N_2 na Ar: průtok Ar v odtahovém plynu (modrá čára) vykazuje oproti signálu nosného plynu (červená čára) zpožděnou a plynulejší odezvu, což je způsobeno transportem a mícháním plynů v odtahovém systému plynu. (b) Křivka normalizovaného průtoku Ar naměřeného v odtahovém plynu [16]

As shown in **Fig. 3(a)**, the plant operation includes a lift-gas switch from N_2 to Ar. By comparing the Ar signal in the off-gas (blue line) with the Ar input signal (red line), a time delay of approximately 57s and a smoother (less steep) output are observed. The Ar output, which represents the step response of the Ar input, is fitted with a curve and corresponding equation shown in **Fig. 3(b)**. To make the rCFD-predicted H_2 mass flow at the melt surface $\dot{m}_{\mathrm{H2,input}}(t)$ comparable to plant measurements, its output at the end of the off-gas stream $\dot{m}_{\mathrm{H2,output}}(t)$ is approximated by using convolution with the system's impulse response $h(t)$:

$$\dot{m}_{\mathrm{H2,output}}(t) = \dot{m}_{\mathrm{H2,input}}(t) * h(t) \tag{4}$$

Here, $h(t)$ is obtained by differentiating the fitted step response $y(t)$.

In **Fig. 4**, a comparison between rCFD predictions and plant measurements of the H_2 mass flow in the off-gas is presented. The rCFD results include the H_2 mass flow rate at the melt surface (blue lines) and the adjusted signal at the end of the off-gas stream (green lines), obtained by applying the transfer function described earlier.

The vacuum chamber pressure, which reduces from atmospheric pressure to around 5mbar during treatment, is also shown (black lines). The two subfigures correspond to different assumptions for calculating the equilibrium hydrogen content $[H]_e$: (a) using the chamber pressure as a simplification, and (b) using the H_2 partial pressure within the H_2-N_2-Ar gas mixture. It should be noted that case (b) still represents a simplified model and will be refined in future work.

In both cases, the predicted H_2 mass flow curves exhibit an initial rise followed by a gradual decay, which resembles similar main characteristics in comparison with plant data. The applied transfer function introduces a noticeable time delay and smoothing effect, aligning the simulation more closely with the measurement.

Hutnické listy – *Metallurgical Journal*
Speciální vydání / Special Issue, roč. / vol. LXXIX
ISSN Online: 3029-8350

However, the initiation of hydrogen degassing differs between the two cases due to the distinct equilibrium conditions arising from the different pressure assumptions. This leads to variations in the overall degassing behavior.

Given that the majority of the vacuum chamber is expected to be filled with the lift-gas Ar, using the H_2 partial pressure within the H_2–N_2–Ar gas mixture likely provides a more realistic representation on the degassing process.

Nonetheless, further refinement of the model is required to more accurately estimate the equilibrium hydrogen content. In comparison with plant data, a notable discrepancy remains: the total amount of H_2 detected in the off-gas is significantly lower in the plant measurements than predicted by simulations.

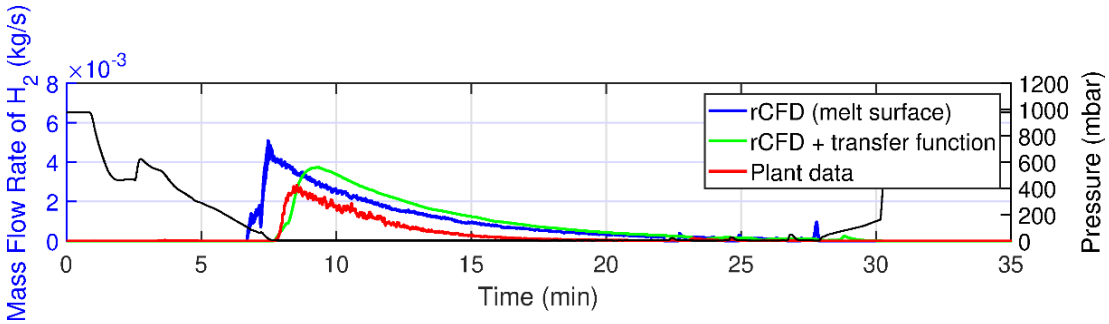

(a)

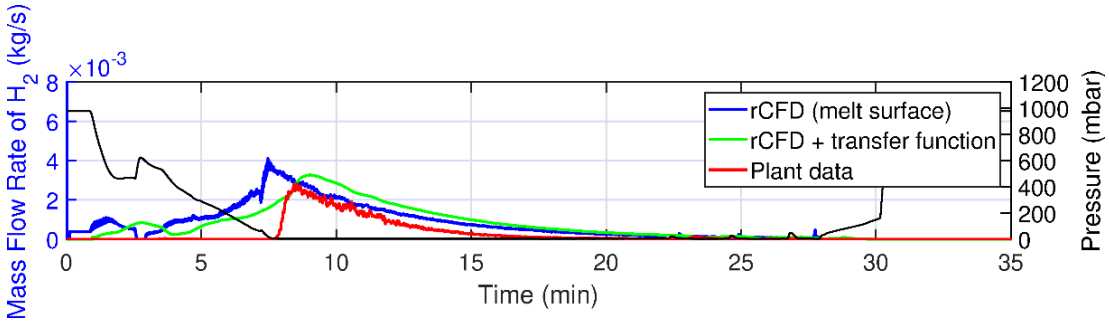

(b)

Fig. 4 Comparison between rCFD predictions and plant measurements of H_2 mass flow rate in the off-gas. Both rCFD-predicted H_2 mass flow at the melt surface (bule line) and the corresponding signal after applying the transfer function (green line) are shown, along with the operating pressure (black line). In (a), the chamber pressure is used to calculate equilibrium H concentration for simplification, while (b) presents results using the H_2 partial pressure, accounting for the H_2-N_2-Ar gas mixture

Obr. 4 Porovnání predikcí z rCFD a měření hmotnostního průtoku H_2 v odtahovém plynu provedených v provozních podmínkách. Jsou zde znázorněny jak hmotnostní průtok H_2 na povrchu taveniny predikovaný metodou rCFD (modrá čára), tak odpovídající signál po použití přenosové funkce (zelená čára), spolu s provozním tlakem (černá čára). V případě (a) se pro zjednodušení používá tlak v komoře k výpočtu rovnovážné koncentrace H, zatímco (b) představuje výsledky s použitím parciálního tlaku H_2, zohledňujícího směs plynů H_2-N_2-Ar

To further quantify hydrogen loss, the concentration of dissolved hydrogen in the steel before and after RH vacuum treatment is analysed. As shown in **Fig. 5**, the hydrogen loss determined from melt measurements closely matches the rCFD predictions. Minor discrepancies may stem from the assumption of a higher total steel mass in simulation compared to the actual ladle. In contrast, the hydrogen loss derived from the integral off-gas analysis is more than twice as low.

Hutnické listy – *Metallurgical Journal*
Speciální vydání / Special Issue, roč. / vol. LXXIX
ISSN Online: 3029-8350

Seemingly, at the plant, some hydrogen is 'lost' on the way to the final monitoring point. The underlying cause of this mass discrepancy remains uncertain. One hypothesis is that some hydrogen reacts with ambient oxygen in hot regions of the off-gas piping to form water vapor. This possibility is currently under investigation, with the aim of ensuring a reliable off-gas hydrogen signal for validating rCFD predictions.

Meanwhile, further improvement of the degassing model implementation in rCFD is essential to more accurately simulate the process. With proper validation, the real-time capable rCFD approach can be extended to support additional metallurgical processes, such as alloying.

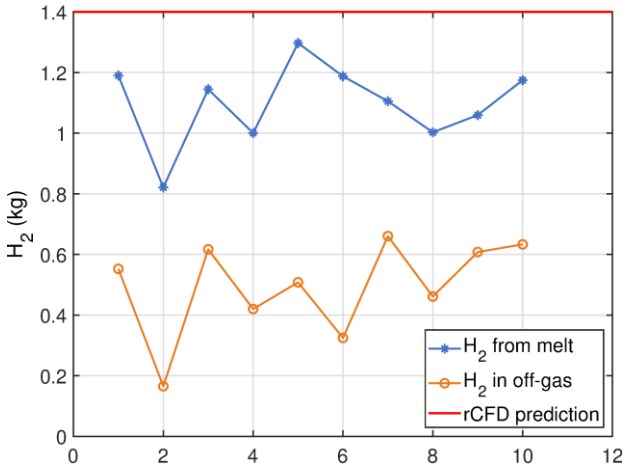

Fig. 5 Comparison of hydrogen mass loss from the melt estimated by: (1) difference in hydrogen concentration in the melt before and after RH treatment (blue markers, based on analysis of multiple melts), (2) integration of H_2 mass flow rate measured in the off-gas (orange markers), and (3) integration of H_2 mass flow rate predicted by rCFD simulations (red line). The H_2 content estimated from the off-gas analysis is significantly lower than that determined from melt measurements

Obr. 5 Srovnání úbytku vodíku (kg) z taveniny stanoveného na základě: (1) rozdílu v koncentraci vodíku v tavenině před a po zpracování na RH stanici (modrá křivka, analyzováno více tavenin), (2) integrace hmotnostního průtoku H_2 naměřeného v odtahovém plynu (oranožová křivka), a (3) integrace hmotnostního průtoku H_2 predikovaného rCFD simulacemi (červená čára). Obsah H_2 stanovený z analýzy odtahového plynu je výrazně nižší než obsah stanovený na základě měření taveniny.

4. Conclusion

- In this study, transport-based rCFD was applied to predict hydrogen degassing in an RH plant. Comparison with plant measurements of hydrogen in the off-gas shows that rCFD predictions qualitatively agree well with the plant data, while also offering real-time capable performance.
- To achieve quantitative alignment, further work should address uncertainties in hydrogen mass loss measurements and ensure accurate model implementation – particularly in the calculation of hydrogen partial pressure under degassing conditions.
- With validation established based on the hydrogen degassing case, the rCFD framework can be further extended to simulate additional metallurgical processes in the RH plant, such as alloying and decarburization. Ultimately, this paves the way for employing rCFD as a digital twin monitoring tool for efficient RH process operation.

Hutnické listy – *Metallurgical Journal*
Speciální vydání / Special Issue, roč. / vol. LXXIX
ISSN Online: 3029-8350

Acknowledgements

The authors gratefully acknowledge the funding support of K1-MET GmbH, metallurgical competence center. The research program of the competence center K1-MET is supported by COMET (Competence Center for Excellent Technologies), the Austrian program for competence centers.

COMET is funded by the Federal Ministry for Transport, Innovation and Technology, the Federal Ministry for Science, Research and Economy, the province of Upper Austria, Tyrol, and Styria, the Styrian Business Promotion Agency.

The authors moreover gratefully acknowledge financial support from the Austrian Research Promotion Agency (FFG) for the project OpTwinFlow (program "Produktion und Material", project number FO999899007).

References

[1] PIRKER, Stefan, PUTTINGER, Stefan, RÖSSLER, Roman and LICHTENEGGER, Thomas. Steel alloy homogenization during Rheinsahl–Heraeus Vacuum Treatment: Conventional computational fluid dynamics, recurrence computational fluid dynamics, and Plant Observations. Steel Research International, 2020, 91(12). DOI 10.1002/srin.202000214.

[2] HAAS, Tim, SCHUBERT, Christian, EICKHOFF, Moritz and PFEIFER, Herbert. Numerical modelling of the ladle flow by a les-based Eulerian–Lagrange Approach: A systematic survey. Metallurgical and Materials Transactions B, 2021, 52(2), pp. 903–921. DOI 10.1007/s11663-021-02064-2.

[3] LI, Baokuan and TSUKIHASHI, Fumitaka. Modelling of circulating flow in rh degassing vessel water model designed for two- and multi-legs operations. ISIJ International, 2000, 40(12), pp. 1203–1209. DOI 10.2355/isijinternational.40.1203.

[4] GENG, Dian-Qiao, ZHENG, Jin-Xing, WANG, Kai, WANG, Ping, LIANG, Ru-Quan, LIU, Hai-Tao, LEI, Hong and HE, Ji-Cheng. Simulation on decarburization and inclusion removal process in the ruhrstahl–heraeus (RH) process with ladle bottom blowing. Metallurgical and Materials Transactions B, 2015, 46(3), pp. 1484–1493. DOI 10.1007/s11663-015-0314-1.

[5] LING, Haitao, LI, Fei, ZHANG, Lifeng and CONEJO, Alberto N. Investigation on the effect of nozzle number on the recirculation rate and mixing time in the rh process using VOF + DPM model. Metallurgical and Materials Transactions B, 2016, 47(3), pp. 1950–1961. DOI 10.1007/s11663-016-0669-y.

[6] CHEN, Gujun, WANG, Qiangqiang and HE, Shengping. Computational fluid dynamics modelling of argon–steel (–slag) multiphase flow in an Ruhrstahl–Heraeus Degasser: A review of past numerical studies. Steel Research International, 2022, 94(1). DOI 10.1002/srin.202200298.

[7] LICHTENEGGER, T. and PIRKER, S. Recurrence CFD – a novel approach to simulate multiphase flows with strongly separated time scales. Chemical Engineering Science, 2016, 153, pp. 394–410. DOI 10.1016/j.ces.2016.07.036.

[8] PIRKER, S. and LICHTENEGGER, T. Efficient time-extrapolation of single- and multiphase simulations by transport based recurrence CFD (rCFD). Chemical Engineering Science, 2018, 188, pp. 65–83. DOI 10.1016/j.ces.2018.04.059.

[9] LUMETZBERGER, H., PIRKER, S. and LICHTENEGGER, T. Propagator-moments approximation for recurrence CFD: Application to species transport in turbulent flows. Chemical Engineering Science, 2025, 311, pp. 121624. DOI 10.1016/j.ces.2025.121624.

[10] LICHTENEGGER, T., PETERS, E.A.J.F., KUIPERS, J.A.M. and PIRKER, S. A recurrence CFD study of heat transfer in a fluidized bed. Chemical Engineering Science, 2017, 172, pp. 310–322. DOI 10.1016/j.ces.2017.06.022.

[11] LICHTENEGGER, T., KIECKHEFEN, P., HEINRICH, S. and PIRKER, S. Dynamics and long-time behavior of gas–solid flows on recurrent-transient backgrounds. Chemical Engineering Journal, 2019, 364, pp. 562–577. DOI 10.1016/j.cej.2019.01.161.

[12] DABBAGH, Firas, PIRKER, Stefan and SCHNEIDERBAUER, Simon. A fast modelling of chemical reactions in industrial-scale olefin polymerization fluidized beds using recurrence cfd. AIChE Journal, 2021, 67(5). DOI 10.1002/aic.17161.

[13] DU, Yaxing, BLOCKEN, Bert and PIRKER, Stefan. A novel approach to simulate pollutant dispersion in the built environment: Transport-based recurrence CFD. Building and Environment, 2020, 170, pp. 106604. DOI 10.1016/j.buildenv.2019.106604.

[14] PIRKER, S., AIGNER, A. and WIMMER, G. Experimental and numerical investigation of sloshing resonance phenomena in a spring-mounted rectangular tank. Chemical Engineering Science, 2012, 68(1), pp. 143–150. DOI 10.1016/j.ces.2011.09.021.

[15] WEI, Ji-He and YU, Neng-Wen. Mathematical modelling of decarburisation and degassing during vacuum circulation refining process of molten steel: Mathematical Model of the process. Steel Research International, 2002, 73(4), pp. 135–142. DOI 10.1002/srin.200200185.

[16] THUMFART, Maria, ZHANG, Xiaomeng, GRUBER, Christine, WACHLMAYR, Johann, PIRKER, Stefan and RÖSSLER, Roman. Making rh fit for green steel production: A multi-method approach to process monitoring. BHM Berg- und Hüttenmännische Monatshefte, 2025. DOI 10.1007/s00501-025-01593-6.